Journal of Materials Chemistry A

Accepted Manuscript

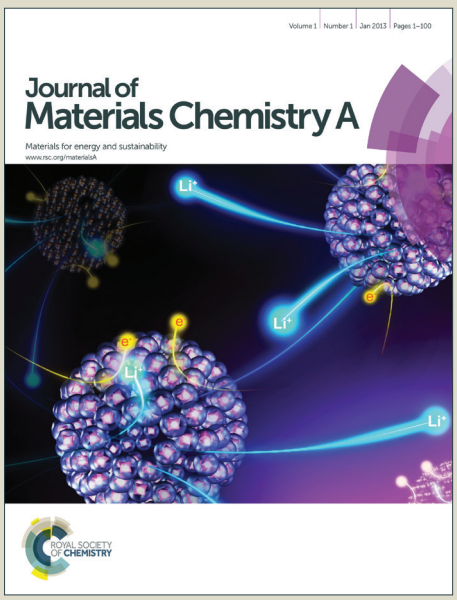

ROYAL SOCIETY OF CHEMISTRY

www.rsc.org/materialsA

$CoSe_2$ Necklace-like Nanowires Supported by Carbon Fiber Paper: A 3D Integrated Electrode for Hydrogen Evolution Reaction

Ke Wang[a], Dan Xi[a], Chongjian Zhou[a], Zhongqi Shi[a*], Hongyan Xia[a], Guiwu Liu[b], Guanjun Qiao[a, b*]

[a] State Key Laboratory for Mechanical Behavior of Materials, Xi'an Jiaotong University, Xi'an 710049, China

[b] School of Materials Science and Engineering, Jiangsu University, Zhenjiang 212013, China

[*] Corresponding author: zhongqishi@mail.xjtu.edu.cn (Z. Shi); gjqiao@mail.ujs.edu.cn (G. Qiao)

ABSTRACT:

Pyrite-type $CoSe_2$ necklace-like nanowires (NWs) were successfully grown on carbon fiber paper (CFP) and proven to be an efficient electrocatalyst towards hydrogen evolution reaction (HER). By combing the use of mesoporous CFP and the nano-structuring of electrocatalyst, the highly active $CoSe_2$ necklace-like NWs on CFP only need the modest overpotentials of 188 and 199 mV to afford the current densities of 50 and 100 mA cm^{-2} respectively. The small Tafel slope of 34 mV dec^{-1} and charge transfer resistance of 7.05 Ω illustrate the prominent electrocatalysis performance. After continual electrolysis for 20 h or conducting cycling for 5000

times, the high activity of $CoSe_2$ NWs toward HER is still perfectly preserved. The outstanding electrocatalysis performance and stability make the $CoSe_2$ necklace-like NWs on CFP a promising earth-abundant electrocatalyst for HER and other renewable energy applications.

Hydrogen as a clean, sustainable alternative fuel is deemed to be a promising solution to the challenges of energy consumption in the future.[1-3] Electrocatalytic as well as photoelectrochemical water splitting in acid electrolyte is the main method to produce hydrogen. Although the noble metal Pt performs excellently in catalysis, the high costs and low reserves severely hamper its practical application.[4] Therefore, the design and synthesis of an advanced material acting as high-performance catalyst for water splitting to replace Pt becomes the key issue and intrigues great interests.[5-7] Many earth-abundant nanomaterials have been successfully synthesized and proven to be candidates as electrocatalysts for hydrogen evolution reaction (HER); a few examples are MoS_2,[8, 9] CoS_2,[10, 11] NiS_2,[10, 12] FeP,[6] $MoSe_2$,[13] Mo_2C[14] and CoSe.[15] However, the reported catalysts still suffered from insufficient activity and poor stability comparing with Pt. Thus, fabricating earth-abundant catalysts of optimal nanostructure with both prominent activity and durability towards HER is still the main challenge.

$CoSe_2$ has two common crystal structures of the cubic pyrite type and orthorhombic marcasite type phases. Due to its unique electronic configuration, the intrinsic metallic nature of $CoSe_2$ ensures the fast charge transport from the electrode surface to the inside part which is an essential property of superior electrocatalysts.[16, 17] $CoSe_2$ has been widely prepared as electrocatalysts for oxygen evolution reaction (OER),[18-20] oxygen reduction reaction (ORR),[21, 22] dye-sensitized solar cells[23] and Li-O_2 batteries.[24] Not until very recently has the $CoSe_2$ been reported as the cathode for HER with distinguished performance. Kong et al.[16] reported the synthesis of $CoSe_2$

nanoparticles grown on carbon fiber paper; Zhang et al.[25] successfully prepared $CoSe_2$ nanoparticles on graphite disk; Xu and Gao with their co-workers combined $CoSe_2$ nanobelts with nickel/nickel oxide nanoparticles[26] or MoS_2[27] to achieve a synergistic effect in HER. However, the published works seldom focused on the nanostructure design of $CoSe_2$, which has been testified to be contributive to HER performances in other electrocatalysts.[6, 11, 28, 29]

Herein, we for the first time report the synthesis of the $CoSe_2$ necklace-like nanowires (NWs) supported by carbon fiber paper (CFP) as an earth-abundant, high-performance and binder-free 3-dimensional (3D) integrated electrode for HER. This electrode with the heterostructure that $CoSe_2$ NWs supported by micron-scale porous CFP has the following merits: (i) $CoSe_2$ exhibits superior HER performance to other transition dichalcogenide electrocatalysts such as MoS_2, WSe_2 for the pristine metallic property;[16, 29] (ii) the necklace-like morphology increases the active sites by exposing larger surface area to the electrolyte; (iii) comparing with common nanoparticles, the nanostructure of NW arrays enjoy the advantages of higher durability and performance by enhancing both the charge transport and hydrogen gas release;[1, 6, 11] (iv) directly growing the NWs onto the 3D substrate of CFP produces a binder-free integrated electrode for HER which avoids the inactive binders and enhances the full use of catalysts.[6, 16, 29] The reported necklace-like $CoSe_2$ NWs on CFP as the integrated cathode for HER displays low overpotential, small Tafel slope and great stability. It has been proven to be an excellent earth-abundant

electrocatalysts for HER.

The synthesis of $CoSe_2$ NWs on CFP could be divided into 2 steps: (i) growth of $Co(OH)(CO_3)_{0.5}$ NWs on CFP hydrothermally; (ii) conversion of $Co(OH)(CO_3)_{0.5}$ NWs to $CoSe_2$ NWs by reacting with selenium vapor (Fig. 1). The XRD pattern of the step 1 products, $Co(OH)(CO_3)_{0.5}$ NWs, is presented in Fig. S1. The pattern of $Co(OH)(CO_3)_{0.5}$ NWs perfectly matches the standard PDF card JCPSD No. 48-0058. The crystal structures of bare CFP and products of step 2 are illustrated by their patterns as shown in Fig. 2(a). According to Fig. 2(a), we found that temperature plays a key role in the selenization process. When performed at 350 °C, the $Co(OH)(CO_3)_{0.5}$ could hardly completely transfer to $CoSe_2$, while the crystalline $CoSe_2$ phase is able to achieve when the selenization temperature is raised to 400 °C and higher. However, further element identification using EDS analysis (Fig. S2) demonstrates that oxygen-free, pure, crystalline $CoSe_2$ (PDF JCPDS No.03-065-3327) could not be reached until the selenization temperature rises to 450 °C. This result is also in agreement with Shi's work.[30] Avoiding the existence of oxygen in the catalyst is crucial, because the cobalt oxide is an inert material toward HER and the oxidization of selenium may cause the dissolving of materials. The chemical composition of $CoSe_2$ NWs could be further confirmed by the XPS analysis. Fig. 2(b) and (c) show the XPS survey of Se 3d and Co 2p regions of $CoSe_2$ NWs. The binding energies of Se $3d_{3/2}$ and $3d_{5/2}$ peaks located at 55.2 eV and 54.5 eV respectively are in good coincidence with the reported data of Se in $CoSe_2$.[16] Moreover, the Co $2p_{1/2}$ and

$Co2p_{3/2}$ centered at 793.3 eV and 778.4 eV also correspond to Co(II) in $CoSe_2$.[16, 25, 31, 32] Thus, it is confirmed that the pure and highly crystalline pyrite-type $CoSe_2$ has been successfully synthesized through the two-step process.

SEM and TEM were used to observe the morphologies of bare CFP (Fig. S3(a) and (b)), $Co(OH)(CO_3)_{0.5}$ NWs (Fig. S4) and $CoSe_2$ NWs supported by CFP (Fig. 3). As $CoSe_2$ NWs selenized at 450 to 600 °C shows the similar morphology, only the typical one is presented here. As revealed in Fig. S3(a), CFP shows a micro-porous structure formed by interconnected carbon fibers. The high electric conductivity, large surface area, smooth electrolyte diffusion tunnels and great mechanical property make CFP the perfect substrate for electrocatalysts,[6, 29] fuel cells[33] and supercapacitors.[34, 35] Fig. S3(b) reveals the detailed surface morphology of an individual carbon fiber. The rough surface of carbon fiber ensures the strong adhesion to $CoSe_2$ NWs which is beneficial to the outstanding durability performance. Fig. 3(a) and (b) show the SEM images of $CoSe_2$ NWs on CFP. As illustrated by the SEM images, the $CoSe_2$ NWs are uniformly covered on every single carbon fiber in a well-aligned pattern. Moreover, from the high-magnification SEM image (Fig. 3(b)) and low-magnification TEM image (Fig. 3(c)), it is clearly observed that the single crystal $CoSe_2$ nanoparticles are joined one by one in line forming a necklace-like NW morphology. The HRTEM image (Fig. 3(d)) taken from a typical $CoSe_2$ NW shows clear grain boundaries and the lattice fringes of (21-1) and (112) planes with the corresponding d-spacing of 0.24 nm. The STEM image and the EDS elemental mappings of $CoSe_2$ NWs testify that the

Co and Se elements are uniformly distributed throughout the whole NW (Fig. S4). For comparisons, the SEM and TEM images of $Co(OH)(CO_3)_{0.5}$ NWs are presented in Fig. S5. The morphology and crystal structure of the $CoSe_2$ are evidently different from $Co(OH)(CO_3)_{0.5}$, whereas the well aligned NW pattern is preserved. Besides, we also found that the necklace-like NW morphology could change to the coral-like morphology (Fig. S6(a) and (b)) when the selenization temperature reached 650 °C due to the fast Oswald ripening. In summary, these results firmly illustrate the formation of cubic pyrite-type $CoSe_2$ necklace-like NWs on CFP. The formation of the necklace-like morphology should be mainly attributed to the fast reaction between the single-crystalline $Co(OH)(CO_3)_{0.5}$ NWs and the highly active selenium vapor.

The catalytic performances of $CoSe_2$ NWs synthesized at different temperatures，bare CFP and 20%wt Pt/C on CFP with identical loading to $CoSe_2$ NWs toward HER were examined in 0.5 M H_2SO_4 using a three-electrode configuration. All the results are presented with *iR*-corrected data and the series resistance R_s was determined by EIS measurements. Fig. 4(a) shows the polarization curves of bare CFP, 20%wt Pt/C on CFP and the $CoSe_2$ NWs on CFP. According to the curves, Pt/C nearly shows zero overpotential and excellent performance, whereas bare CFP exhibits poor activity towards HER and makes negligible contribution to the performances of the integrated electrodes. With respect to the $CoSe_2$ necklace-like NWs on CFP, they all show highly activity toward HER and the electrode synthesized at 450 °C is testified to be the optimal one. To afford the current densities of 10, 30, 50 and 100 mA cm^{-2}, the $CoSe_2$

necklace-like NWs synthesized at 450 °C only require the overpotentials of 165, 181, 188 and 199 mV respectively. Among the $CoSe_2$ NWs/CFP electrodes measurements in our investigation, the ones with the necklace-like morphology (selenized at 450 to 600 °C) exhibit small differences in activity. In order to drive a current density of 100 mA cm^{-2}, the electrodes selenized at 500, 550, 600 °C need the overpotentials of 210, 208, 215 mV respectively. Tafel slope is another key parameter to evaluate the activity of catalysts and smaller Tafel slope means that a lower overpotential is required to afford an interested current density. As illustrated by Fig. 4(b), the small Tafel slopes of the electrodes with the selenization temperature of 450, 500, 550, 600 and 650 °C are 34.0, 35.7, 35.4, 38.3 and 39.8 mV dec^{-1} respectively. The Pt/C shows a very small Tafel slope of 30.4 mV dec^{-1}, which is in coincidence with reported data.[36] The electrode of optimal performance with the Tafel slope of 34.0 mV dec^{-1} is also among the best electrocatalysts ever reported (Table S1). The Tafel slopes lower than 40 mV dec^{-1} suggests that the HER takes place through the Volmer-Heyrovsky route, in which the rate-limiting step is the electrochemical recombination between the chemisorbed H and another proton.[37-39] All these results suggest the similar surface chemistry and nanoscaled morphology of the samples synthesized at 600 °C and below, as these catalysts are prepared by the same process. However, the relatively low selenization temperature could help to reserve more defects and nanoscaled roughness, which have been proved to be capable of promoting catalytic activity and ensuring a larger accessible area.[7, 19, 29] As a result, the sample selenized at 450 °C

possesses a slightly better performance. The catalytic performance of necklace-like $CoSe_2$ NWs toward HER compares favorably to the most recently reported earth-abundant HER catalysts in acid media (Table S1).

However, the sample selenized at 650 °C exhibits a relatively modest performance. With a Tafel slope of 39.8 mV dec^{-1}, the electrode has to require an overpotential of 249 mV to maintain the current density of 100 mA cm^{-2}. In order to quantitatively compare its coral-like morphology (Fig. S6) with the necklace-like one, the double-layer capacity, C_{dl}, is used to determine the electrochemically active surface area. The cyclic voltammetry (CV) was conducted between 0.1 and 0.2 V (vs RHE) at different scan rates to involve the double-layer capacitance only (Fig. S7(a)). By linear fitting the double-layer capacitive currents against scan rates, the C_{dl} of the electrode selenizied at 450 and 650 °C is determined to be 4.02 and 1.57 mF cm^{-2} respectively (Fig. S7(b)), which is comparable to other electrocatalysts with the NW morphology.[6, 29] EIS is believed to be an important technique as a supplement to the characterization of interface reactions and electrode kinetics.[11, 40] As given in the inset of Fig. S8, the equivalent circuit used to fit the EIS experimental data includes a series resistance element R_s, a charge transfer resistance element R_{ct} and a constant phase element (CPE). By fitting the Nyquist plots of $CoSe_2$ synthesized at 450 and 650 °C, the parameters in the equivalent circuit are determined (Fig. S8). Rather than the similar R_s (<2 Ω), the R_{ct} of 7.05 and 69.8 Ω corresponding to the sample synthesized at 450 and 650 °C exhibit the evident difference. Both the higher C_{dl} and lower R_{ct}

illustrate the superior electrocatalytic activity of $CoSe_2$ necklace-like NWs on CFP to the coral-like one synthesized at 650 °C. It is believed that the larger accessible surface area ensured by the unique necklace-like structure and higher intrinsic activity preserved by the low synthesis temperature mainly contribute to the better performance.[25, 41]

The stability is also one of the essential aspects in evaluating electrocatalysts. The stability of $CoSe_2$ NWs on CFP was firstly tested by conducting CV within the potential range of 0.2 to -0.3 V (vs RHE) for 5000 cycles. The lower potential limit was determined to drive a current density of approximately 30 mA cm^{-2}. Fig. 5(a) shows the initial polarization curve and the one after 5000 cycles. It is evident that the highly active nature of the $CoSe_2$ necklace-like NWs on CFP is preserved perfectly and the cathodic current density suffers no loss after 5000 cycles. At the current densities of 10 and 100 mV, the corresponding overpotential increases are only 1 and 2 mV. Besides, the Tafel slope only increases slightly from 34.0 to 36.0 mV dec^{-1} after 5000 cycles, which further confirms the great stability. Moreover, the durability of the electrocatalysts in working situation is also evaluated by electrolysis at a fixed overpotential to drive an initial current density of 50 mA cm^{-2} for 20 h. At the end of the test, the cathodic current density exhibits no current density drop (Fig. 5(b)). The outstanding stability in both the CV cycling and continual electrolysis guarantees its prominent quality in practical applications. The morphology of $CoSe_2$ NWs after stability tests was also examined by SEM (Fig. S9(a) and (b)). The

nano-heterostructure was well maintained after the tests and only the slight bundle-up of NWs is observed due to the surface tension. The excellent stability performance is mainly due to the pure oxygen-free composition and high crystallization, both of which help to eliminate the dissolution of electrocatalysts in acid media.[5, 42]

Conclusions

In summary, we have successfully synthesized the $CoSe_2$ NWs with necklace-like morphology supported by CFP as an earth-abundant, high-performance and binder-free 3D electrode for HER. The unique nanostructure ensures a large contact area with the electrolyte and also enhances the hydrogen gas bubbles release from the surface. In aqueous acid electrolyte, the overpotentials of only 188 and 199 mV are required to drive the current densities of 50 and 100 mA cm^{-2}. The small Tafel slope of 34 mV dec^{-1} ensures that it only needs a small overpotential to afford a large current density. After the stability test of conducting CV for 5000 cycles and electrolysis at a fixed potential for 20 h, the necklace-like NW morphology and the prominent activity of the catalyst are perfectly preserved leading to the great stability. The performance of $CoSe_2$ necklace-like NWs on CFP electrode is among the best of the earth-abundant electrocatalysts ever reported. The integrated electrode with optimal micro and nano structuring $CoSe_2$ has been proven to be an advanced catalyst for HER and other renewable energy applications.

Acknowledgements

This work was supported by the Key Grant Project of Chinese Ministry of Education (313046), the National Natural Science Foundation of China (51202181) and the Program for New Century Excellent Talents in University (NCET-12-0454).

References

1. C. G. Morales-Guio, L. A. Stern and X. Hu, *Chem. Soc. Rev.*, 2014, **43**, 6555-6569.
2. A. B. Laursen, S. Kegnæs, S. Dahl and I. Chorkendorff, *Energ. Environ. Sci.*, 2012, **5**, 5577.
3. D. Kong, J. J. Cha, H. Wang, H. R. Lee and Y. Cui, *Energ. Environ. Sci.*, 2013, **6**, 3553.
4. J. R. McKone, S. C. Marinescu, B. S. Brunschwig, J. R. Winkler and H. B. Gray, *Chem. Sci.*, 2014, **5**, 865.
5. Y. Li, Y. Yu, Y. Huang, R. A. Nielsen, W. A. Goddard, Y. Li and L. Cao, *ACS Catal.*, 2015, **5**, 448-455.
6. Y. Liang, Q. Liu, A. M. Asiri, X. Sun and Y. Luo, *ACS Catal.*, 2014, **4**, 4065-4069.
7. H. Du, S. Gu, R. Liu and C. M. Li, *J. Power Sources*, 2015, **278**, 540-545.
8. X. Zheng, J. Xu, K. Yan, H. Wang, Z. Wang and S. Yang, *Chem. Mater.*, 2014, **26**, 2344-2353.
9. D. Wang, Z. Pan, Z. Wu, Z. Wang and Z. Liu, *J. Power Sources*, 2014, **264**, 229-234.
10. M. S. Faber, M. A. Lukowski, Q. Ding, N. S. Kaiser and S. Jin, *J. Phys. Chem. C*, 2014, **118**, 21347-21356.
11. M. S. Faber, R. Dziedzic, M. A. Lukowski, N. S. Kaiser, Q. Ding and S. Jin, *J. Am. Chem. Soc.*, 2014, **136**, 10053-10061.
12. H. Pang, C. Wei, X. Li, G. Li, Y. Ma, S. Li, J. Chen and J. Zhang, *Sci. Rep.*, 2014, **4**, 3577.
13. D. Kong, H. Wang, J. J. Cha, M. Pasta, K. J. Koski, J. Yao and Y. Cui, *Nano Lett.*, 2013, **13**, 1341-1347.
14. H. Vrubel and X. Hu, *Angew. Chem. Int. Ed.*, 2012, **51**, 12703-12706.
15. A. I. Carim, F. H. Saadi, M. P. Soriaga and N. S. Lewis, *J. Mater. Chem. A*, 2014, **2**, 13835.
16. D. Kong, H. Wang, Z. Lu and Y. Cui, *J. Am. Chem. Soc.*, 2014, **136**, 4897-4900.
17. H. Sato, F. Nagasaki, Y. Kani, S. Senba, Y. Ueda, A. Kimura and M. Taniguchi, *Surf. Rev. Lett.*, 2002, **09**, 1315-1319.
18. Y. R. Zheng, M. R. Gao, Q. Gao, H. H. Li, J. Xu, Z. Y. Wu and S. H. Yu, *Small*, 2015, **11**, 182-188.
19. Y. Liu, H. Cheng, M. Lyu, S. Fan, Q. Liu, W. Zhang, Y. Zhi, C. Wang, C. Xiao, S. Wei, B. Ye and Y. Xie, *J. Am. Chem. Soc.*, 2014, **136**, 15670-15675.
20. M. R. Gao, Y. F. Xu, J. Jiang, Y. R. Zheng and S. H. Yu, *J. Am. Chem. Soc.*, 2012, **134**, 2930-2933.
21. M.-R. Gao, S. Liu, J. Jiang, C.-H. Cui, W.-T. Yao and S.-H. Yu, *J. Mater. Chem.*, 2010, **20**, 9355.
22. H. Li, D. Gao and X. Cheng, *Electrochim. Acta*, 2014, **138**, 232-239.
23. H. Sun, L. Zhang and Z.-S. Wang, *J. Mater. Chem. A*, 2014, **2**, 16023-16029.

24. S. Dong, S. Wang, J. Guan, S. Li, Z. Lan, C. Chen, C. Shang, L. Zhang, X. Wang, L. Gu, G. Cui and L. Chen, *J. Phys. Chem. Lett.*, 2014, **5**, 615-621.
25. H. Zhang, L. Lei and X. Zhang, *RSC Adv.*, 2014, **4**, 54344-54348.
26. Y. F. Xu, M. R. Gao, Y. R. Zheng, J. Jiang and S. H. Yu, *Angew. Chem. Int. Ed.*, 2013, **52**, 8546-8550.
27. M. R. Gao, J. X. Liang, Y. R. Zheng, Y. F. Xu, J. Jiang, Q. Gao, J. Li and S. H. Yu, *Nat. Commun.*, 2015, **6**, 5982.
28. L. Zhang, K. Xiong, S. Chen, L. Li, Z. Deng and Z. Wei, *J. Power Sources*, 2015, **274**, 114-120.
29. K. Xu, F. Wang, Z. Wang, X. Zhan, Q. Wang, Z. Cheng, M. Safdar and J. He, *ACS nano*, 2014, **8**, 8468-8476.
30. J.-B. Shi, P.-F. Wu, C.-T. Kao, M.-W. Lee, C.-C. Chan, P.-C. Yang, C.-L. Lin, R.-Y. Huang, Y.-J. Huang, S.-K. Lin, F.-C. Cheng, H.-S. Lin and H.-W. Lee, *Cryst. Res. Technol.*, 2015, **50**, 1-5.
31. S. Lauer, A. Trautwein and F. Harris, *Phys. Rev. B*, 1984, **29**, 6774-6783.
32. S. Miyahara and hei, *J. Appl. Phys.*, 1968, **39**, 896.
33. X. Zhang and Z. Shen, *Fuel*, 2002, **81**, 2199-2201.
34. A. Banerjee, S. Bhatnagar, K. K. Upadhyay, P. Yadav and S. Ogale, *ACS Appl. Mater. Inter.*, 2014, **6**, 18844-18852.
35. K. Wang, Z. Shi, Y. Wang, Z. Ye, H. Xia, G. Liu and G. Qiao, *J. Alloys Compd.*, 2015, **624**, 85-93.
36. J. Kibsgaard and T. F. Jaramillo, *Angew. Chem. Int. Ed. Engl.*, 2014, **53**, 14433-14437.
37. Y. Zheng, Y. Jiao, M. Jaroniec and S. Z. Qiao, *Angew. Chem. Int. Ed.*, 2015, **54**, 52-65.
38. E. Santos, P. Quaino and W. Schmickler, *Phys. Chem. Chem. Phys.*, 2012, **14**, 11224-11233.
39. B. E. Conway and B. V. Tilak, *Electrochim. Acta*, 2002, **47**, 3571-3594.
40. L. Liao, J. Zhu, X. Bian, L. Zhu, M. D. Scanlon, H. H. Girault and B. Liu, *Adv. Funct. Mater.*, 2013, **23**, 5326-5333.
41. M. A. Lukowski, A. S. Daniel, F. Meng, A. Forticaux, L. Li and S. Jin, *J. Am. Chem. Soc.*, 2013, **135**, 10274-10277.
42. J. Deng, P. Ren, D. Deng and X. Bao, *Angew. Chem. Int. Ed.*, 2015, **54**, 2100-2104.

Figures:

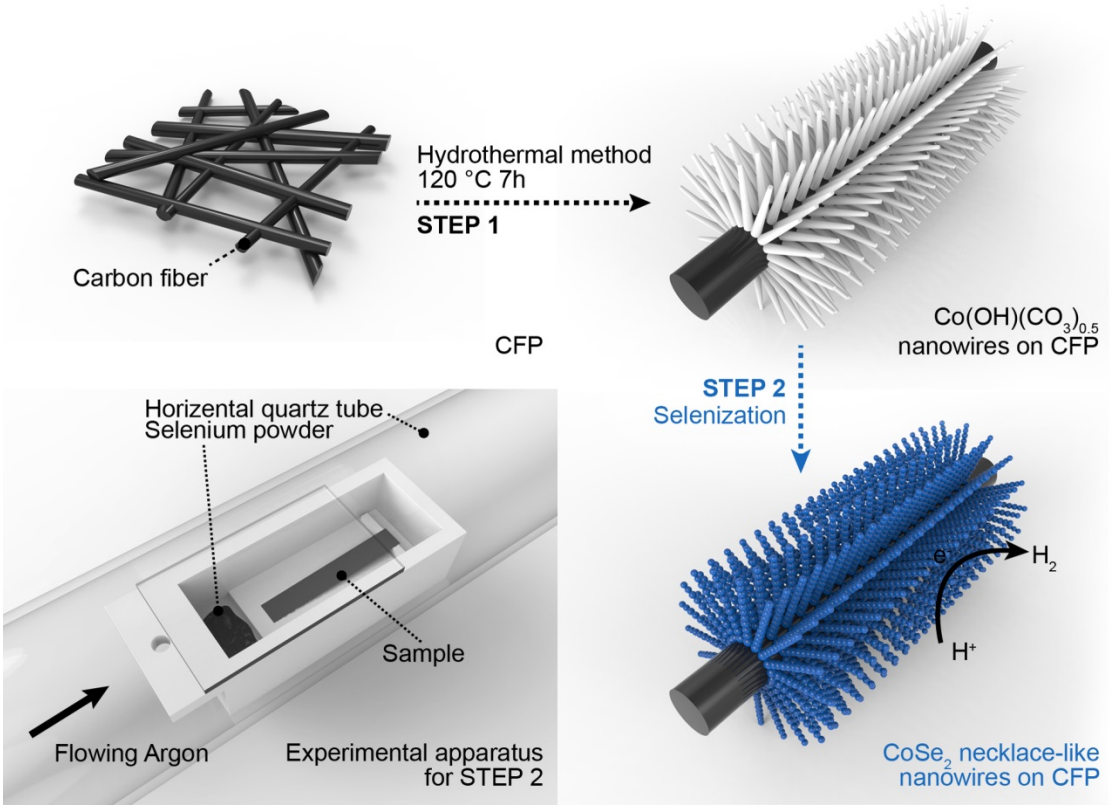

Fig. 1. Schematic illustration of the preparation process of $CoSe_2$ necklace-like NWs on CFP. The inset exhibits the apparatus used in the selenization step schematically.

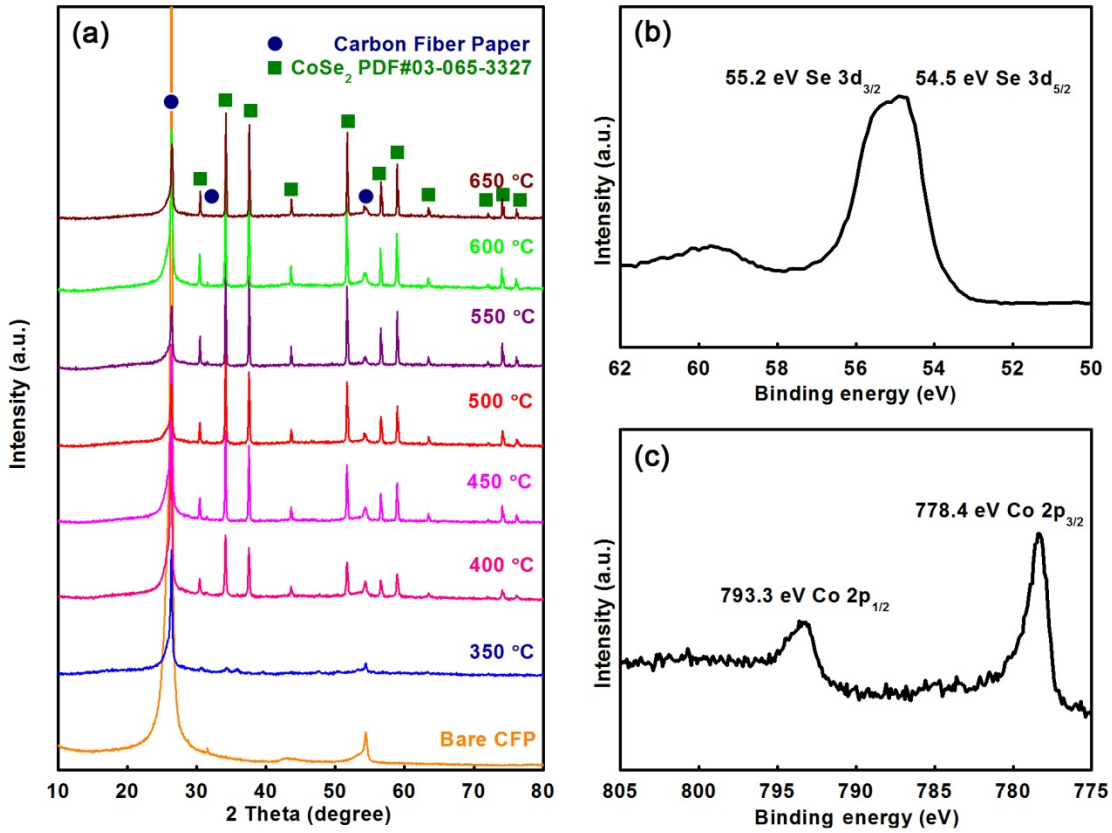

Fig. 2. (a) XRD patterns of bare CFP and samples selenized at 350 to 650 °C. XPS survey of (b) Se 3d and (c) Co 2p regions.

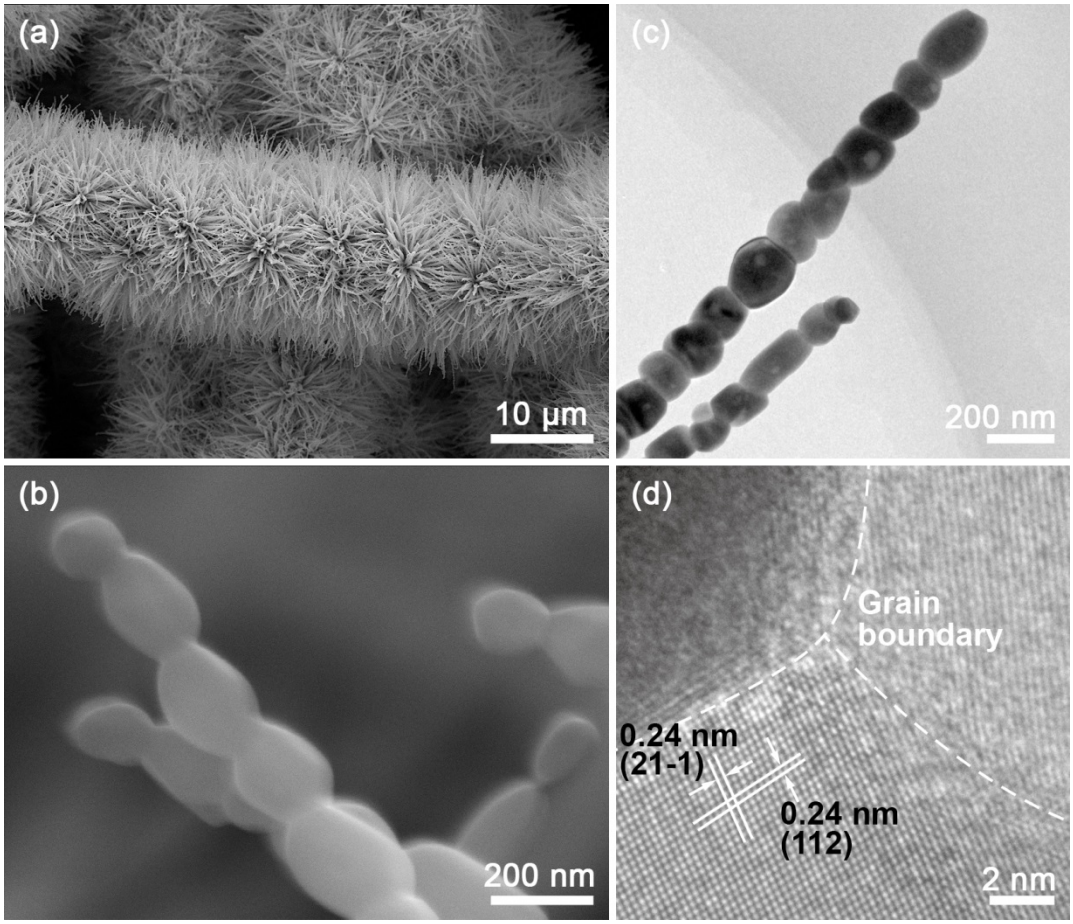

Fig. 3. SEM images (a, b) and TEM images (c, d) of the necklace-like $CoSe_2$ NWs on CFP (selenized at 450 °C).

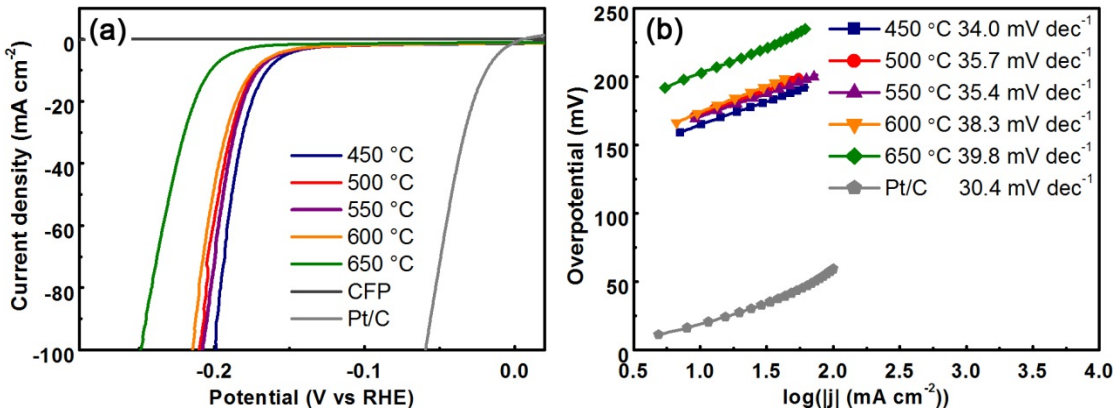

Fig. 4. (a) Polarization curves for bare CFP, 20%wt Pt/C on CFP and $CoSe_2$ NWs on CFP synthesized at different temperatures. (b) Tafel plots for 20%wt Pt/C and $CoSe_2$

NWs on CFP synthesized at different temperatures.

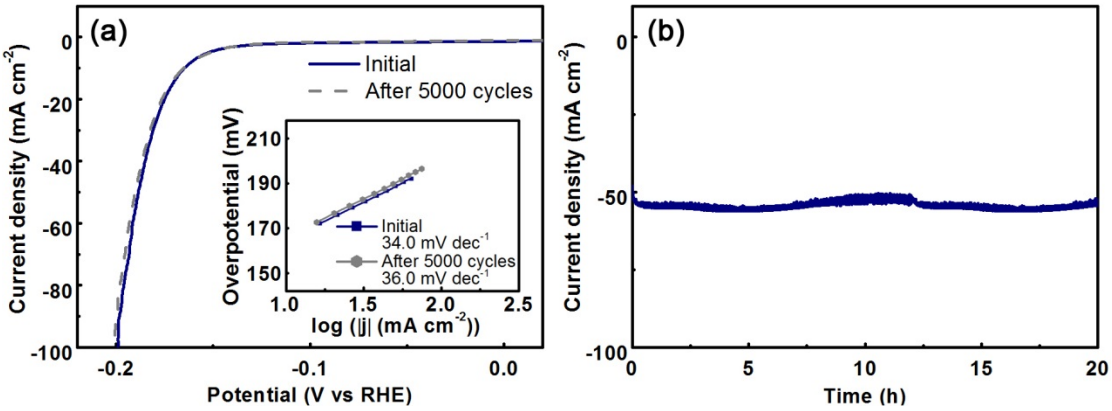

Fig. 5. Stability tests of (a) $CoSe_2$ necklace-like NWs on CFP selenized at 450 °C with initial LSV polarization curve (line) and the one after 5000 cycles (dash); (b) continual electrolysis for 20 h at the fixed overpotential to produce a current density of 50 mA. The inset of Fig. 5(a) shows the corresponding Tafel plots before and after 5000 cycles.

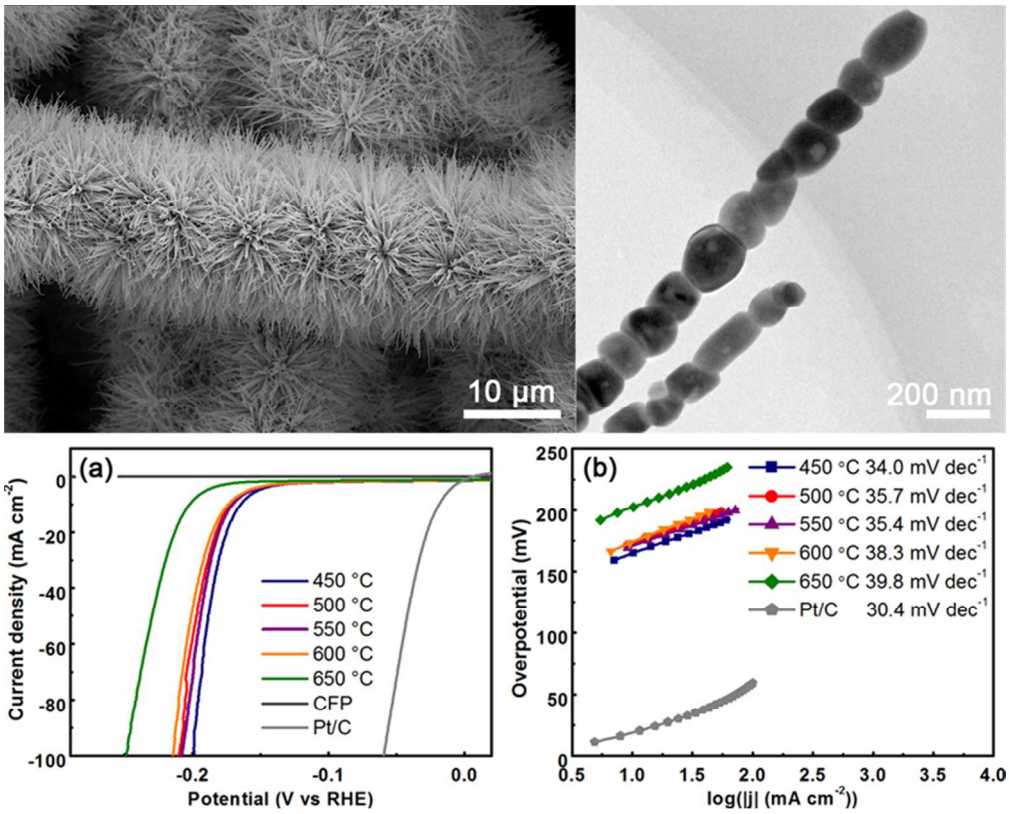

70x56mm (300 x 300 DPI)